

# Nanometer spot allocation for Raman spectroscopy on ferroelectrics by polarization and piezoresponse force microscopy

G. Tarrach,<sup>a)</sup> P. Lagos L., and R. Hermans Z.

Facultad de Física, Pontificia Universidad Católica de Chile, Av. Vicuña Mackenna 4860, 6904411 Santiago, Chile

F. Schlaphof, Ch. Loppacher, and L. M. Eng

Institut für Angewandte Photophysik, Technische Universität Dresden, Mommsenstrasse 13, D-01062 Dresden, Germany

(Received 30 April 2001; accepted for publication 20 August 2001)

We report the 100% correlation between polarized light microscopy (PLM), piezoresponse force microscopy (PFM), and micro-Raman spectroscopy when investigating domain-rich ferroelectric systems. In order to allocate the desired spot on a submicrometer scale, both PLM and PFM were combined to elucidate the effective three-dimensional ferroelectric domain distribution. With PFM we observe spike-like *a* and *c* domains well inside extended *a* and *c*-polarized areas, which were not conclusive with PLM. The knowledge on such a domain distribution is essential when addressing quantitative micro-Raman spectroscopy. In addition, we show the unambiguous differentiation between *a* and *c* domains on the submicrometer scale using the  $B_2$  mode of lattice vibrations. © 2001 American Institute of Physics. [DOI: 10.1063/1.1414292]

Assigning Raman peaks in domain-rich ferroelectric materials so far seems to be an unsolvable problem, since even micro-Raman inspections are probing a sample volume of  $2\text{--}3\ \mu\text{m}^3$  in total,<sup>1</sup> integrating over several ferroelectric polarization directions. The proper Raman data interpretation thus needs a parallel and thorough inspection of the domain distribution. We report on such an approach by combining polarized light microscopy (PLM) and piezoresponse force microscopy (PFM). While PLM gives good results on bulk ferroelectrics covering the regime from 1 mm down to the diffraction limit, PFM is applicable between 100  $\mu\text{m}$  and a few nanometers.<sup>2–4</sup> In most PLM work reported on ferroelectrics an optical contrast is formed by birefringence for optically transparent crystals in transmission,<sup>5,6</sup> and by birefringence, specular reflection or etching in reflected light.<sup>7</sup> Unfortunately, PLM reveals no contrast for domains of anti-parallel polarization unless we apply an external mechanical or electrical stress field. Since such a procedure may influence the domain distribution, we rather prefer the noninvasive method of PFM for this inspection.

In the present study we use Remeika<sup>8</sup> grown BaTiO<sub>3</sub> single crystals of 40  $\mu\text{m}$  thickness. PLM images were taken with an Olympus BHSP polarization microscope using DPlan 4 PO (4 $\times$  magnification, NA 0.10) and DPlan 10 PO (10 $\times$ , 0.25) objective lenses. Both the in-plane and out-of-plane polarization were recorded with a scanning force microscope (SFM) operated in the piezoresponse mode (PFM).<sup>2–4</sup> Applying an alternating voltage (49 kHz, 1.5 V<sub>rms</sub>) to the *p*-doped Si-cantilever tip ( $k=3\ \text{N/m}$ ,  $f_0=70\ \text{kHz}$ ) generates vibrations in the ferroelectric sample via the converse piezoelectric effect, which then are demodulated from the beam deflection signal using conventional lock-in techniques. The micro-Raman spectrograph (Dilor LabRam 010)

is operated with a linearly polarized HeNe laser (632.8 nm, 20 mW) in backscattering geometry using an Olympus MPlan 50 $\times$ , NA 0.75 objective lens. The inelastically scattered light is diffracted without polarization analysis from a 1800 g/mm grating in a 300 mm focal length spectrograph. Sample locations of interest are allocated by using nonpolarized transmission microscopy within the Raman microscope.

Figure 1 compares the results obtained by transmitted light microscopy (a) and PLM (b) from the same area on the BaTiO<sub>3</sub> single crystal. The PLM image is dominated by broad dark *c* domains having the ferroelectric polarization along the [001] direction. Bright areas are attributed to *a* domains where the difference in refractive index between the *c* and *a* axis causes birefringence. Most of these stripes run along the [010] axis. By reasons of minimizing the internal stress, the polarization vector within these *a* domains is aligned along the [100] direction.

Figure 1(b) distinguishes between two main features among the bright areas: (i) *a* domains with a homogeneously colored central part having rainbow-colored sidebands are

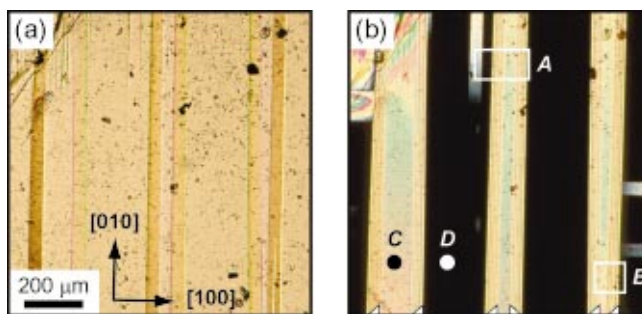


FIG. 1. (Color) Optical transmission (a) and PLM (b) images of the same area on a 40- $\mu\text{m}$ -thick BaTiO<sub>3</sub> single crystal. Stripes of *a* domains within the dark *c* domain are revealed in PLM, while the transmission image shows the dark ferroelastic domain walls. Regions A–D refer to PFM and Raman measurements and the white triangles mark the rainbow-colored sidebands.

<sup>a)</sup>Author to whom correspondence should be addressed; electronic mail: gtarrach@fis.puc.cl

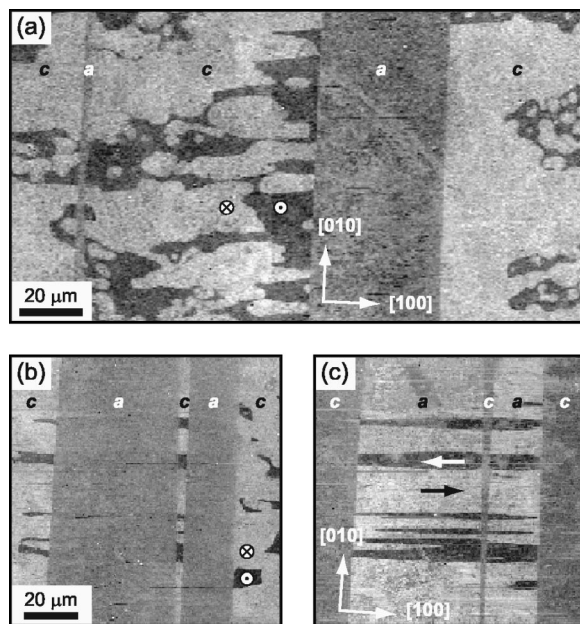


FIG. 2. (a) Composition of two overlapping PFM images of region A in Fig. 1; (b) and (c) of region B. (a) and (b) show the [001] component of ferroelectric polarization with antiparallel  $c$  domains revealed in a black-to-white contrast and  $a$  domains appearing gray. Image (c) displays the [100] component simultaneously recorded with (b), where antiparallel  $a$  domains appear in black and white and the  $c$  domains in gray.

found to be broad  $a$  domains, which penetrate through the whole  $\text{BaTiO}_3$  crystal; and (ii) gray colored  $a$  domains that do not present the rainbow at the border are understood as being very thin  $a$  domains.<sup>5</sup> Therefore, the rainbow-colored sidebands correspond to the  $45^\circ$  wedges that are formed by ferroelastic (101) and ( $\bar{1}01$ ) domain walls, which also produce the dark contrast in the transmission image of Fig. 1(a). This interpretation is supported by the fact that all sidebands measure  $40 \pm 4 \mu\text{m}$  in width corresponding to the crystal thickness. The thin  $a$  domains, however, are too thin to exhibit the sidebands, but we notice that the left border appears sharp when setting the optical focus to the bottom surface of the crystal, and correspondingly for the right border on the top surface. Hence, it becomes clear that also the thin  $a$  domains run at  $45^\circ$  through the crystal.

Although the former inspection gives a clear differentiation of  $a$  and  $c$  domains, we still have no hint about the existence of ferroelectric  $180^\circ$  domain walls within these regions. With PFM we obtain an excellent contrast between domains of inverse polarity. Figures 2(a) and 2(b) show the [001] component (out of plane) of the polarization vector. Black and white represent  $c$  domains of opposite polarity (up/down) while gray corresponds to an  $a$  domain contrast. Figure 2(c) is the [100] component simultaneously recorded with Fig. 2(b). Here, black and white represent opposite in-plane polarity (left/right) and gray corresponds to the  $c$  domains.

In Fig. 2(a) we see that the  $a$  domain of region A measures  $40 \mu\text{m}$  in width, which fits exactly to the central part of the stripe in Fig. 1. At a distance of  $72 \mu\text{m}$  to the left we find another extremely narrow  $a$  domain. Its location corresponds to the right border of the thin  $a$  domain in Fig. 1 if we assume the left ferroelastic domain wall of the broad  $a$  domain to be a ( $\bar{1}01$ ) plane. This assumption is supported by

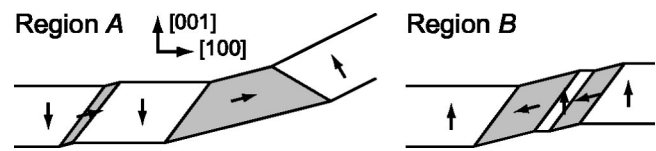


FIG. 3. Schematic model showing the sample topography and ferroelectric domain distribution for cross sections at regions A and B in Fig. 1. The [001] direction is shown highly exaggerated and antiparallel domain structures are not considered.

the simultaneously observed fold in the topography as sketched in Fig. 3, which is caused by the tetragonal distortion of the crystal. This model was verified when inspecting also the bottom surface of the  $\text{BaTiO}_3$  crystal. We confirmed the width of the broad domain and its distance to the thin domain, as well as the fact that both domains are through domains.

From Fig. 2(b) we see that the  $a$ -domain width of  $68 \mu\text{m}$  corresponds to the central part plus one rainbow-colored sideband of the stripe in region B of Fig. 1. Together with the sample topography we conclude the sample cross section to be in accordance with Fig. 3. Furthermore, we observe a narrow  $c$  domain in Figs. 2(b) and 2(c) located within the broad  $a$  domain. The out-of-plane and in-plane images demonstrate that the ferroelectric ( $180^\circ$ ) domain walls in the  $a$  domain are nearly parallel to the [100] direction and that they match the  $180^\circ$  walls in the adjacent  $c$  domains. Again, this is explained by the energetically favorable behavior to avoid charged domain walls.

With the full knowledge on the present domain structure we are now able to allocate the laser focus for micro-Raman spectroscopy completely within the desired domain type, i.e., within an  $a$  or  $c$  domain. The spectra shown in Fig. 4 were taken at the two spots labeled C and D in Fig. 1. For the  $c$  domain the incident polarization was chosen along the [010] axis. In the  $a$  domains, polarization directions parallel to the crystal  $c$  and  $a$  axis were selected for the top and second spectrum in Fig. 4, respectively. Thus, in our micro-Raman measurements we are able to clearly differentiate between the two domain states, in accordance with similar results reported previously.<sup>9</sup> The eminent difference, though, stems from the fact that we need not use any polarization analysis

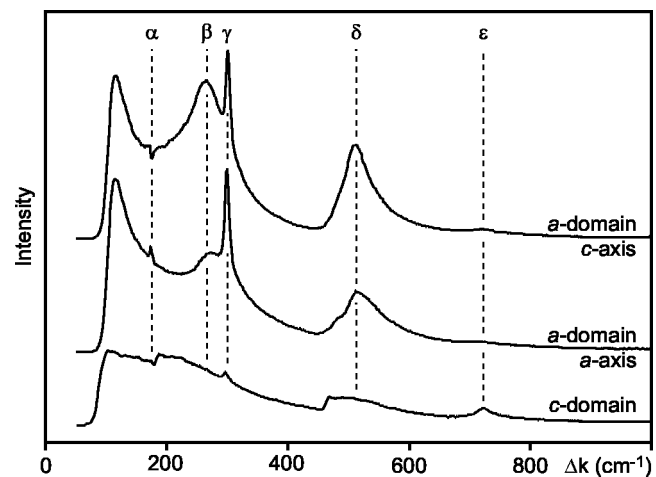


FIG. 4. Micro-Raman spectra of  $a$  and  $c$  domains recorded at spots C and D in Fig. 1. Incident light is [010] polarized in  $c$  domains and along the indicated axes in  $a$  domains.

for data disentangling but simply apply a thorough knowledge on the sample structure and its domain conditions, both obtained from PLM and PFM measurements.

The Raman data in Fig. 4 illustrate two broad peaks, labeled  $\beta$  and  $\delta$ , at 200–300  $\text{cm}^{-1}$  and slightly above 500  $\text{cm}^{-1}$ , respectively, which are reported not to vanish above  $T_C$ . The narrow peak  $\gamma$  at 300  $\text{cm}^{-1}$  is also present in all spectra, but the line named  $\varepsilon$  at 725  $\text{cm}^{-1}$  is very weak in the  $a$ -domain spectra. The latter two peaks are typical for the tetragonal phase of  $\text{BaTiO}_3$  and indicate that the crystal is in its ferroelectric state. Nevertheless, the spectra are sufficiently distinct in order to identify the domain type. Furthermore, the qualitative difference between the two polarization directions within  $a$  domains regarding peak  $\alpha$  at 175  $\text{cm}^{-1}$  allows us to conclude about the direction of the  $c$  axis in the case of an unknown  $a$ -domain orientation.

Although the micro-Raman inspections were performed without polarized detection, the spectra in Fig. 4 clearly show the distinct differences in  $a$  and  $c$  domains. Peak  $\varepsilon$  corresponds to the  $B_2$  phonon mode, which should be absent in  $a$  domains due to the coupling tensors in our Raman geometry.<sup>10</sup> Nevertheless, a small cross talk is visible in our  $a$ -domain spectra, which is attributed to depolarization effects in the focus of the high-NA objective.<sup>1</sup> In contrast to previous work,<sup>11</sup> where positions within “light” or “dark” regions were allocated, we are able to exactly specify the domain type under investigation, as well as to eliminate cross talk from neighboring domain states. Furthermore, previous work on macroscopic crystals showed that the sample history is essential when attributing phonon modes to the observed spectra:<sup>12</sup> since our  $\text{BaTiO}_3$  samples show a time stable domain pattern on the nanometer scale, which was not even affected by heating or cooling, our measurements do not stem from a multidomain state, or from anisotropic fluctuations of domain states driven by phase transitions,<sup>12</sup> relaxation processes, or induced stress<sup>11</sup> or strain.<sup>13</sup>

In conclusion, we demonstrated the importance of an exact three-dimensional knowledge of the domain structure

on the submicrometer scale in order to allocate the spot for micro-Raman spectroscopy on ferroelectrics. This was achieved by combining the results of the diffraction-limited optical techniques of Raman spectroscopy and PLM with the nanometer resolution of PFM. However, it must be emphasized that although we are able to position the laser spot perfectly within each domain type ( $a$  or  $c$ ), the information on the antiparallel domains is lost while transferring the sample from PFM to the Raman spectrometer. Future *in situ* combination of these techniques is thus inevitable when heading towards an accurate and fully three-dimensional theoretical and quantitative understanding of phonon modes in  $\text{BaTiO}_3$  and other ferroic crystals on the nanometer scale.

The authors would kindly like to thank T. Otto for technical help. One of the authors (G.T.) acknowledges financial support from FONDECYT for Project No. 1000531 and from FONDEF Project No. D97F1001. One of the authors (L.M.E.) acknowledges the DFG for financial support under Grant No. EN434/2-1.

- <sup>1</sup>D. J. Gardiner and P. R. Graves, *Practical Raman Spectroscopy* (Springer, Berlin, 1989).
- <sup>2</sup>L. M. Eng, H.-J. Güntherodt, G. A. Schneider, U. Köpke, and J. Muñoz Saldaña, *Appl. Phys. Lett.* **74**, 233 (1999).
- <sup>3</sup>L. M. Eng, G. Rosenman, A. Skliar, M. Oron, M. Katz, and D. Eger, *J. Appl. Phys.* **83**, 5973 (1998).
- <sup>4</sup>A. L. Gruverman, A. Pignolet, K. M. Satyalakshmi, M. Alexe, N. D. Zakharov, and D. Hesse, *Appl. Phys. Lett.* **76**, 106 (2000).
- <sup>5</sup>P. W. Forsbergh, Jr., *Phys. Rev.* **76**, 1187 (1949).
- <sup>6</sup>W. J. Merz, *Phys. Rev.* **95**, 690 (1954).
- <sup>7</sup>J. A. Hooton and W. J. Merz, *Phys. Rev.* **98**, 409 (1955).
- <sup>8</sup>J. P. Remeika, *J. Am. Chem. Soc.* **76**, 940 (1954).
- <sup>9</sup>L. H. Robins, D. L. Kaiser, L. D. Rotter, P. K. Schenck, G. T. Stauff, and D. Rytz, *J. Appl. Phys.* **76**, 7487 (1994).
- <sup>10</sup>D. J. Gardiner and P. R. Graves, *Practical Raman Spectroscopy* (Springer, Berlin, 1989), Chap. 2, p. 23.
- <sup>11</sup>Z. Li, C. M. Foster, X.-H. Dai, X.-Z. Xu, S.-K. Chan, and D. J. Lam, *J. Appl. Phys.* **71**, 4481 (1992).
- <sup>12</sup>A. M. Quittet and M. Lambert, *Solid State Commun.* **12**, 1053 (1973).
- <sup>13</sup>M. Osada, M. Kakihana, S. Wada, T. Noma, and Cho Woo-Seok, *Appl. Phys. Lett.* **75**, 3393 (1999).